Electronic Supplementary Material (ESI) for Journal of Materials Chemistry B.

Supplementary information

Competitive coordination assembly of light-degradable gold nanoclusters-intercalated metal organic frameworks for photoresponsive drug release

Ke Wang,* [a] Sicheng Zhai,[a] Yuanyuan Qin,[b] Mengke Hao,[b] Siqi Su,[b] Shuming Li,*[b] and Xuexue Tang[a]

[a] School of Medical Engineering, Haojing College of Shaanxi University of Science & Technology, Xianyang 712046, Shaanxi, P.R. China

[b] Co-construction Collaborative Innovation Center for Chinese Medicine Resources Industrialization by Shaanxi & Education Ministry, Shaanxi University of Chinese Medicine, Xianyang, 712083, Shaanxi, P.R. China

*Corresponding author

E-mail: iamkwang@163.com; 1501034@sntcm.edu.cn

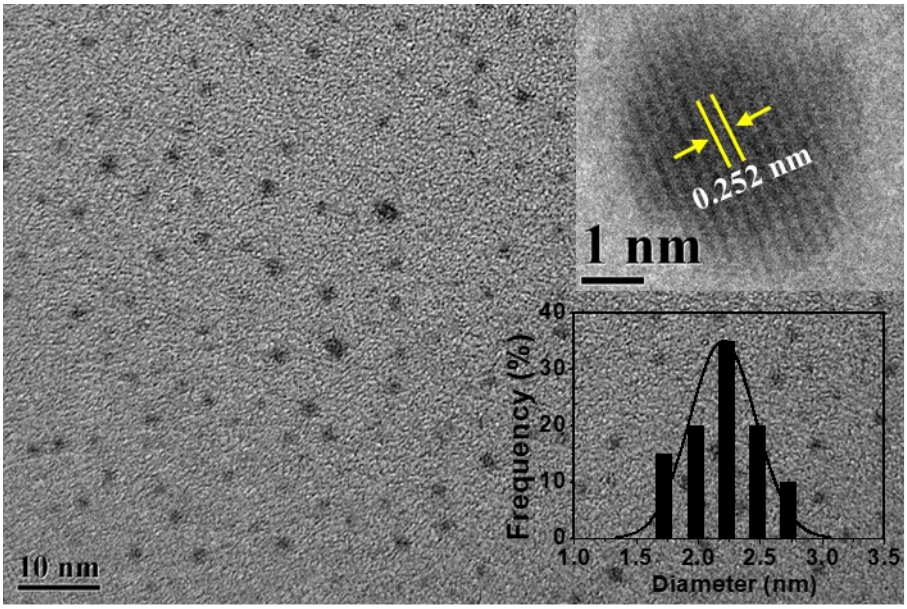

Fig. S1 TEM image of the AuNCs, inset: HRTEM image and size distribution of AuNCs.

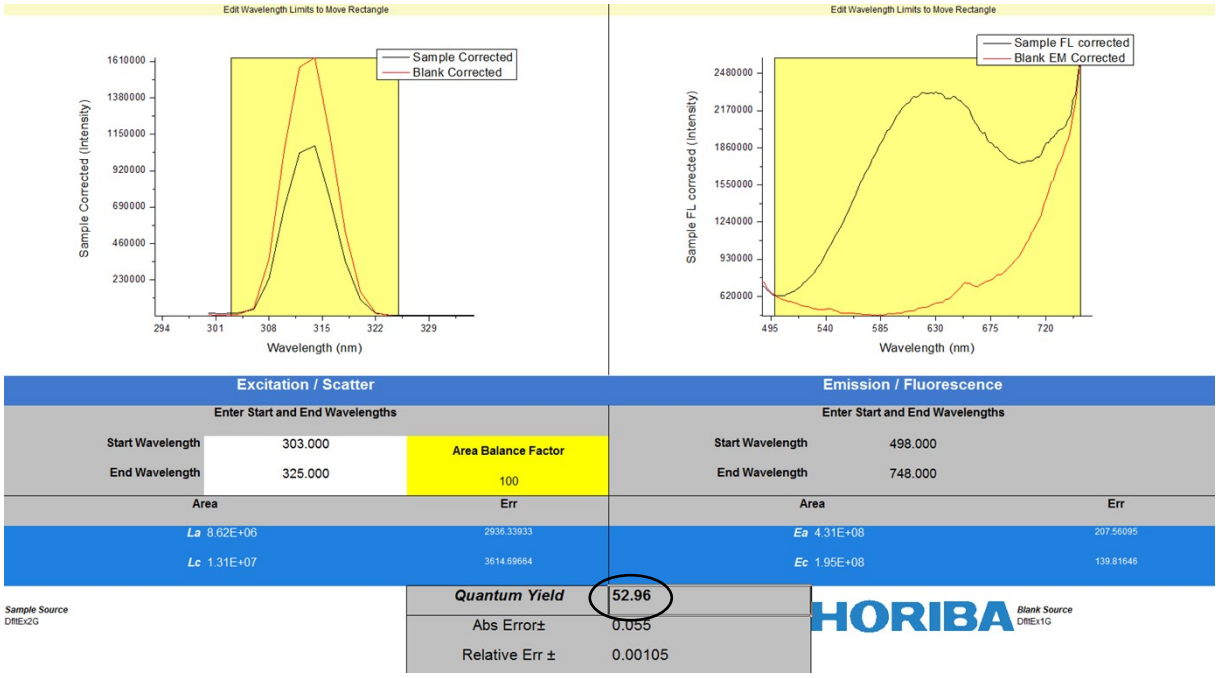

Fig. S2 The QY of AuNC@ZIF-8 in water.

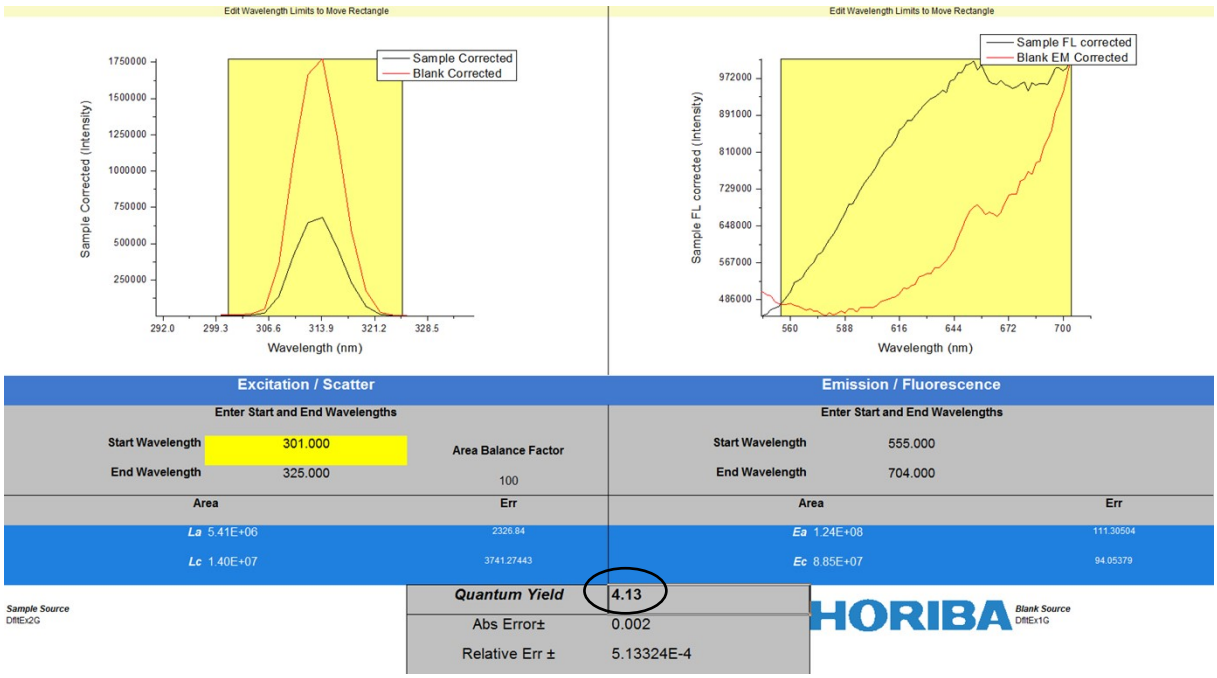

Fig. S3 The QY of AuNCs aqueous solution.

Table S1 List of reported for enhancing QY of GSH-AuNCs.

Materials	Step number	Solution	QY_{AuNCs} (%)	$QY_{material}$ (%)	Ref.
Au NCs/LDH UTFs	Two	H_2O	2.69	14.11	[1]
Au NCs/ELDH	Three	Formamide	2.60	19.05	[2]
Au(I)-Thiolate@SiO_2	Two	85% Ethanol	/	/	[3]
aAuNCs-MOF	Two	Methanol	4.63	7.74	[4]
AuNCs@ZIF-8	Two	Methanol	7.6	33.6	[5]
AuNCs@ZIF-8.	One	H_2O	4.13	52.96	This work

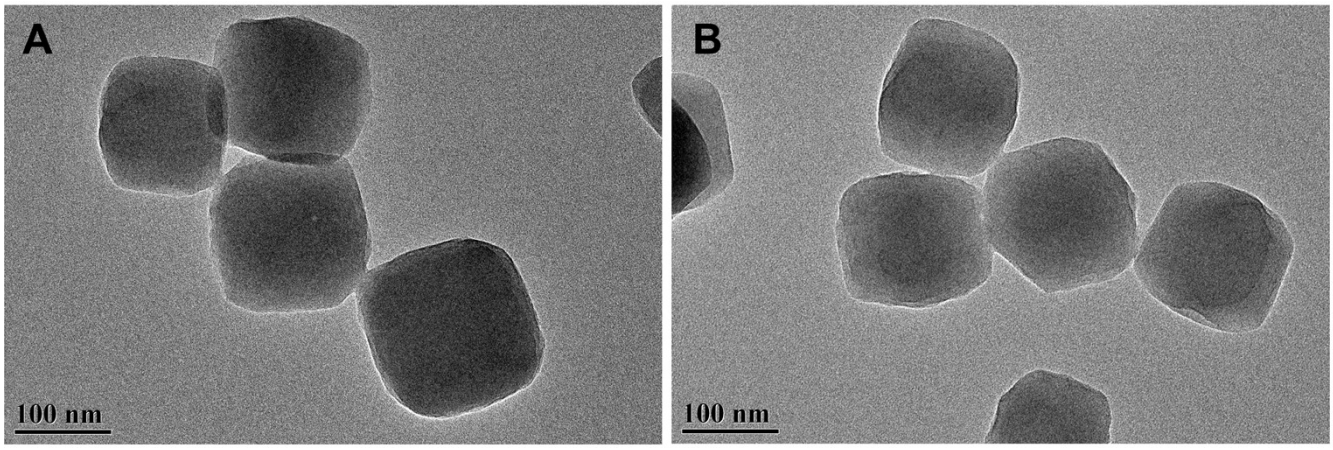

Fig. S4 TEM images of ZIF-8 in water (A) before and (B) after light irradiation at 405 nm (0.1 W/cm^2) for 20 min.

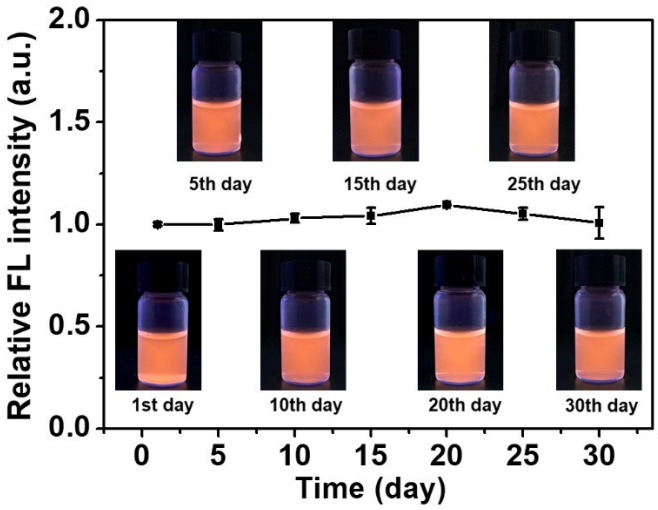

Fig. S5 Relative fluorescence intensity and photographs of AuNC@ZIF-8 aqueous solution for different days.

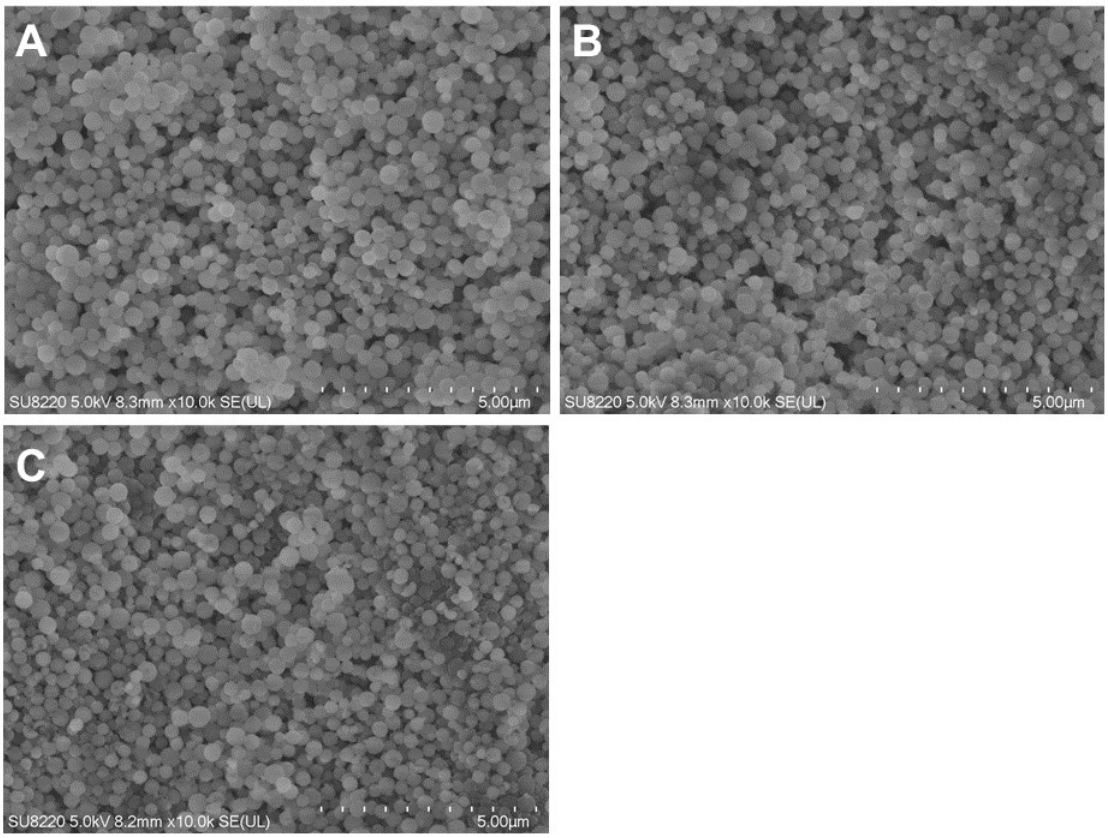

Fig. S6 The SEM images of AuNC@ZIF-8 (A) before and after dispersion in aqueous solution (B) and cell culture medium (C) for 30 days at 4°C.

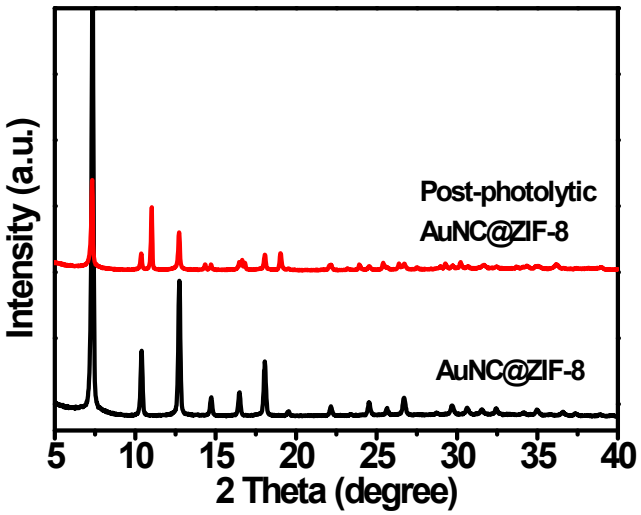

Fig. S7 XRD patterns of AuNC@ZIF-8 and post-photolytic AuNC@ZIF-8.

Table S2 List of XPS area percentage of Au, S, N, O.

	Au		S	N			O
	Au(I)	Au(0)	-SH	$-NH_2$	N-Zn	pyrrolic/N	O-Zn
AuNCs	47.89%	52.11%	15.65%	39.73%	0	60.27	0
post-photolytic AuNCs	31.25%	68.75%	43.59%	N.D.	N.D.	N.D	0
AuNC@ZIF-8	49.41%	50.59%	12.41%	3.58%	51.76%	44.65%	4.59%
post-photolytic AuNC@ZIF-8	34.30%	65.70%	36.59%	0	58.07%	41.93%	15.25%

N.D.: no detection.

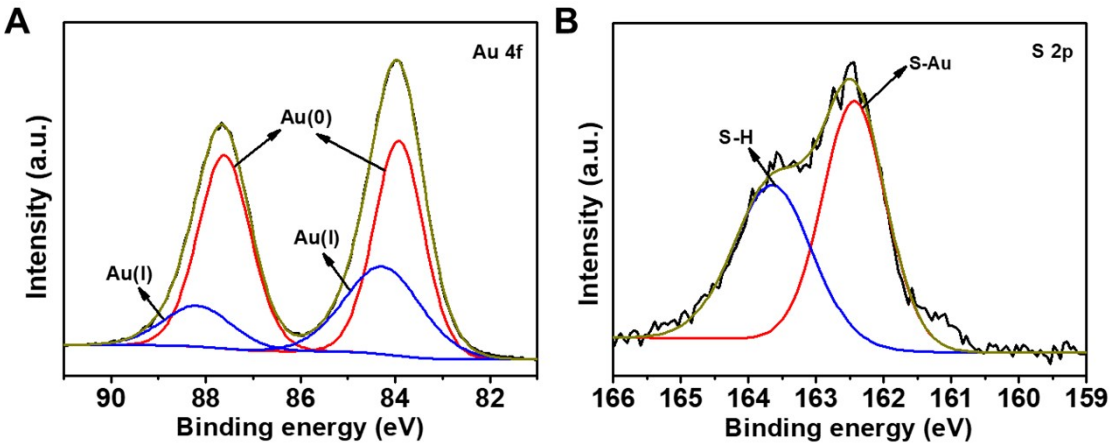

Fig. S8 High-resolution XPS Au 4f (A) and S 2p (B) spectra of the AuNCs aqueous solution after irradiation for 20 min.

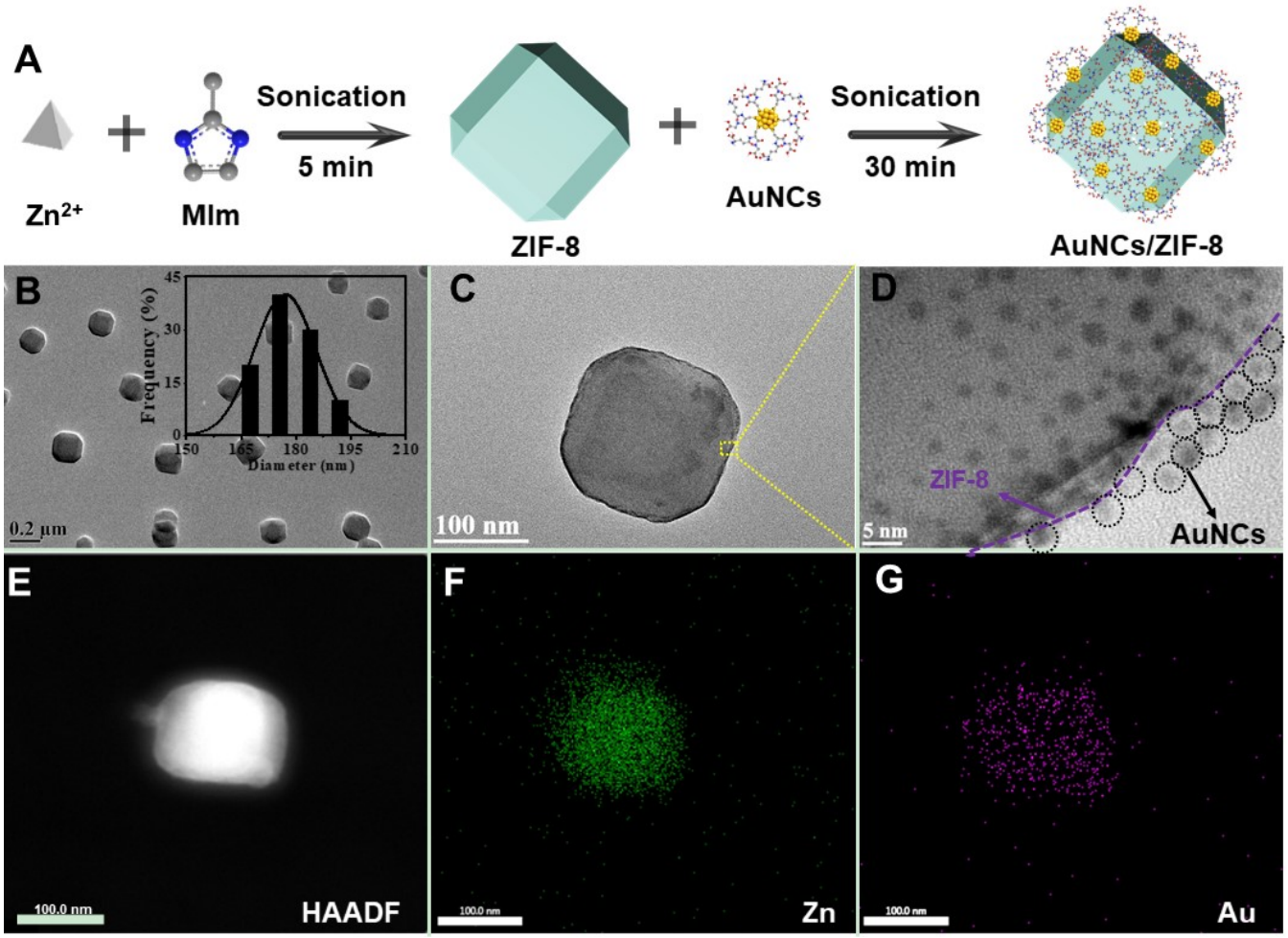

Fig. S9 (A) Schematic illustration of two step synthesis of AuNC/ZIF-8. (B) TEM image of the ZIF-8, inset: size distribution of ZIF-8. (C) TEM image of AuNC/ZIF-8, (D) HRTEM image of the interested district of AuNC/ZIF-8, (E-G) HAADF-STEM images and corresponding elemental mappings of AuNC/ZIF-8.

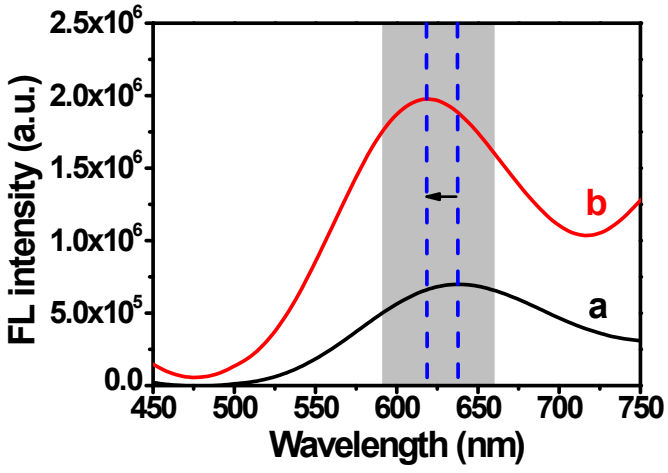

Fig. S10 The fluorescence spectra of the AuNCs (a) and AuNC/ZIF-8 (b).

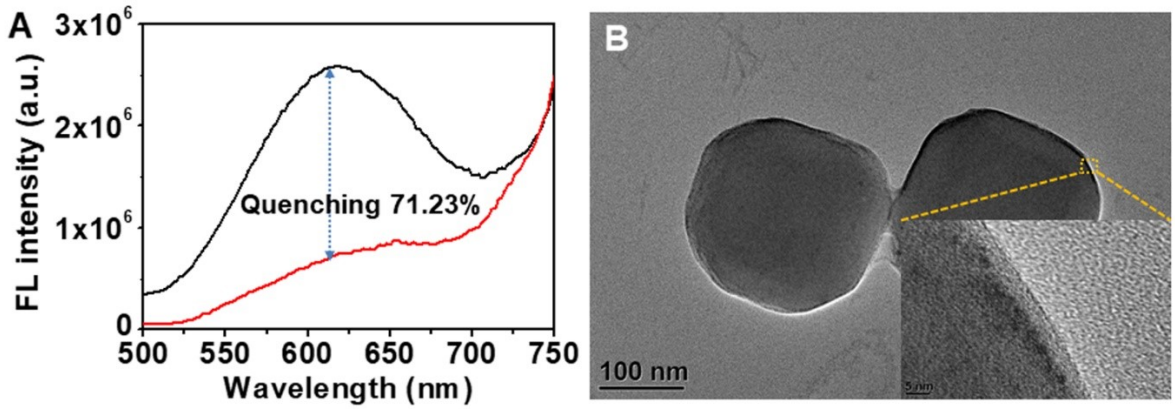

Fig. S11 (A) Fluorescence spectra of the AuNCs/ZIF-8 before (black) and after (red) after irradiation (405 nm) in aqueous solution for 20 min. (B) TEM image of AuNCs/ZIF-8 after light irradiation (405 nm) in aqueous solution for 20 min. inset: HRTEM image of the interest district in B.

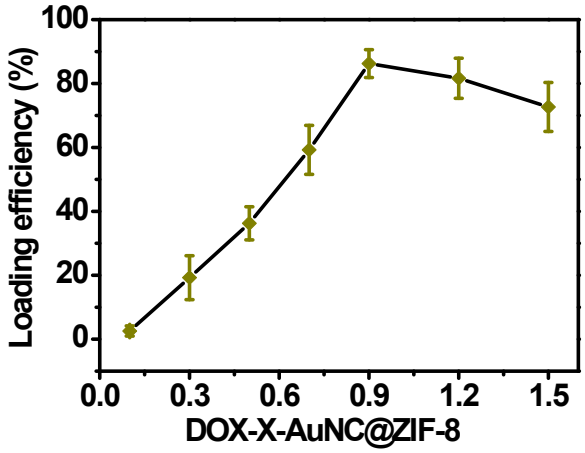

Fig. S12 The loading efficiency of DOX in X-AuNC@ZIF-8.

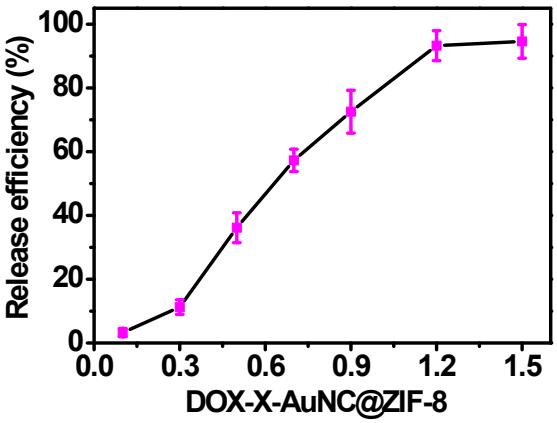

Fig. S13 The release efficiency of DOX-X-AuNC@ZIF-8.

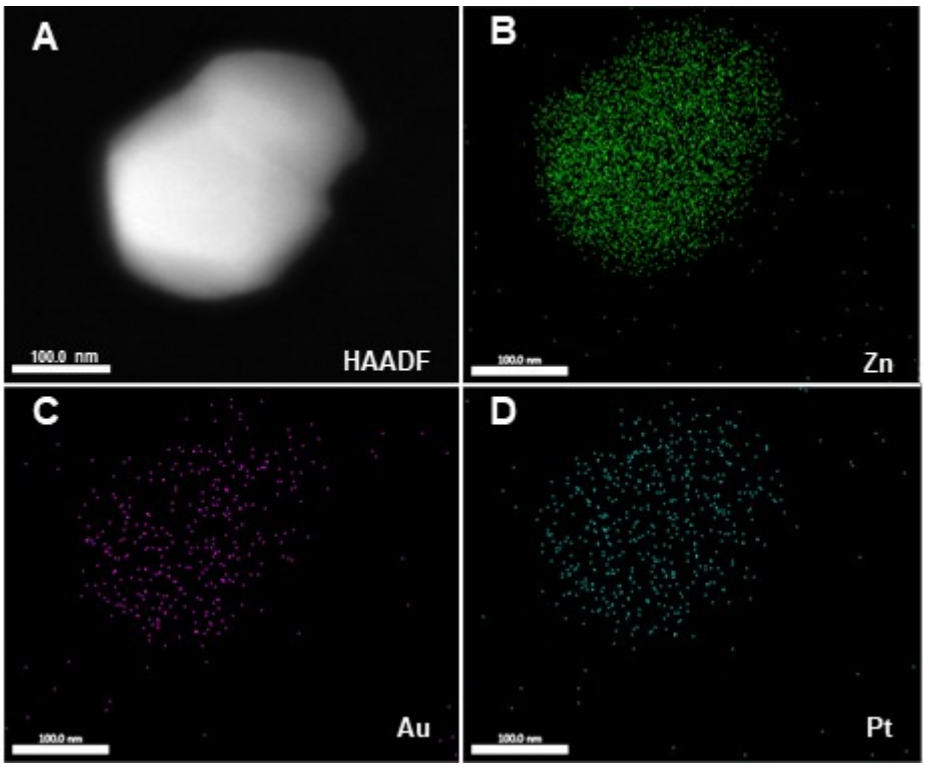

Fig. S14 HAADF-STEM image (A) and elemental mapping of cisplatin-AuNC@ZIF-8 (B-D).

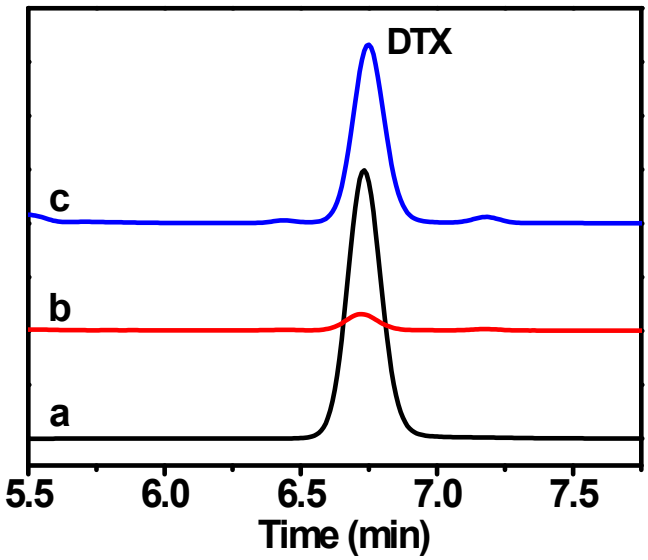

Fig. S15 The HPLC analyses of DTX (UV detection at 243 nm). DTX (a) and the supernatant of DTX-AuNC@ZIF-8 in response to light irradiation (405 nm, 1 W/cm^2) within 0 min (b) and 20 min (c).

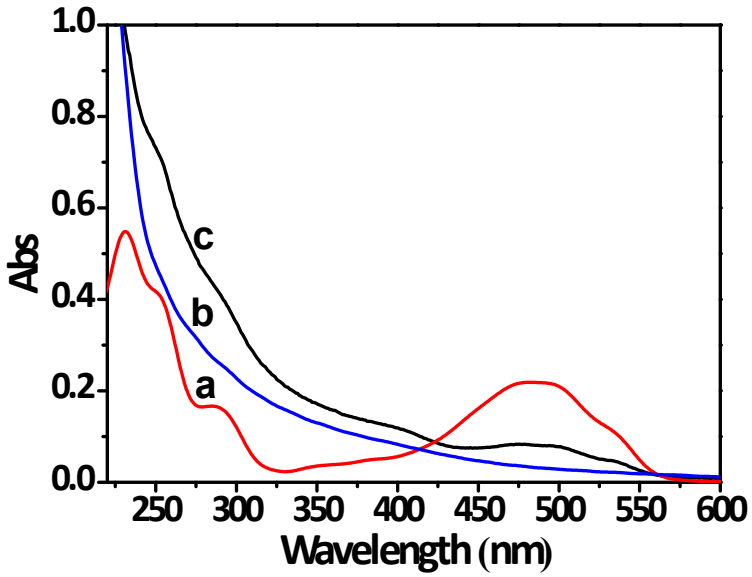

Fig. S16 (A) UV–vis absorption spectra of DOX (a), AuNC@ZIF-8 (b), and DOX-AuNC@ZIF-8 (c).

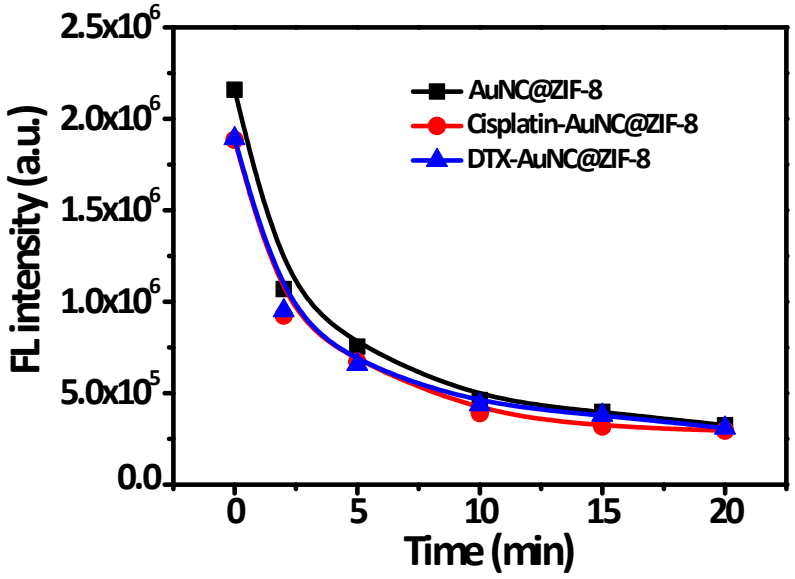

Fig. S17 The fluorescence intensity *vs* irradiation time profiles of AuNC@ZIF-8 and drug-AuNC@ZIF-8.

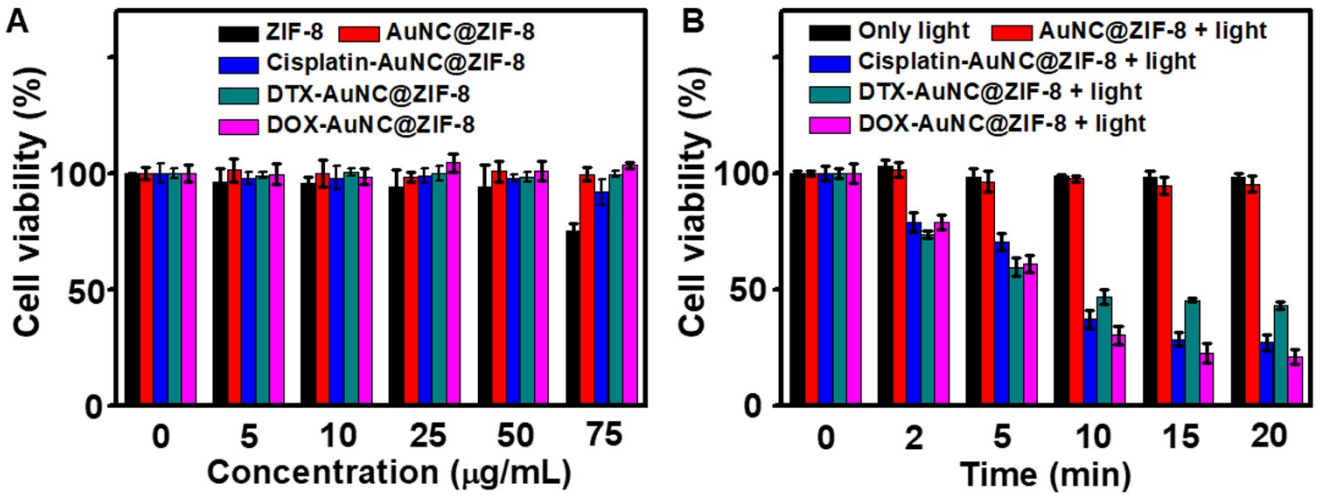

Fig. S18 (A) Cell viability of HeLa cells incubated with different concentrations of ZIF-8, AuNC@ZIF-8 and drug-AuNC@ZIF-8 for 24 h. (B) Cell viability of HeLa cells incubated with 50 μg/mL AuNC@ZIF-8 or 50 μg/mL drug-AuNC@ZIF-8 under different irradiation time.

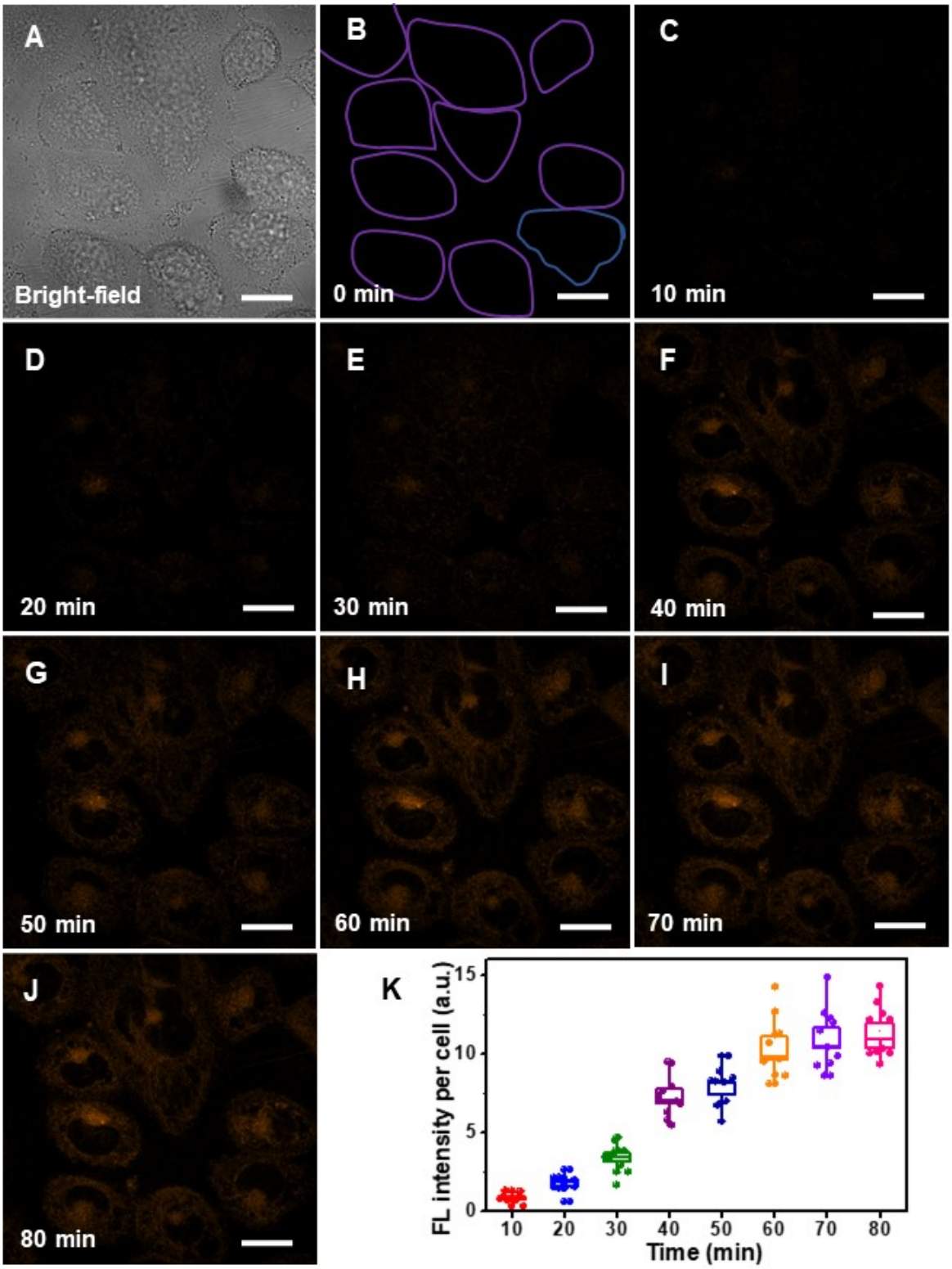

Fig. S19 Bright field image (A) and CLSM image (B) of HeLa cells in the absence of cisplatin-AuNCs@ZIF-8. (C-J) CLSM images of HeLa cells incubated with cisplatin-AuNCs@ZIF-8 for 10 to 80 min. Scale bar: 20 μm. (K) The corresponding intracellular fluorescence intensity of HeLa cells in images C-J. The box plot shows data points, in which each point corresponds to the fluorescence intensity of per cell obtained with ImageJ software.

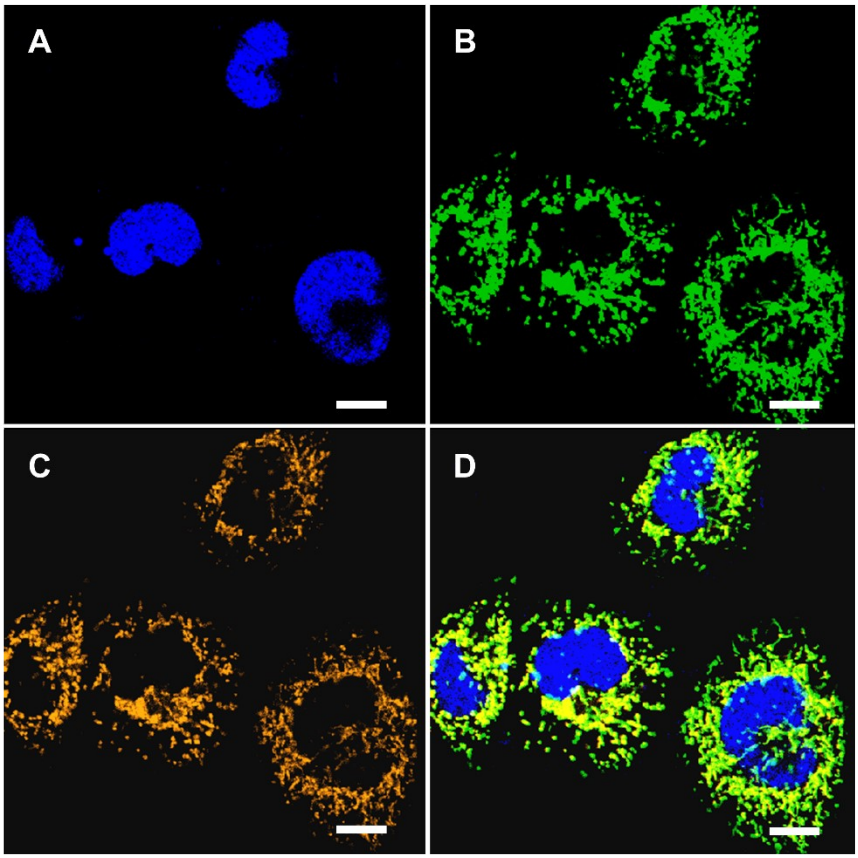

Fig. S20 CLSM images of HeLa cells co-incubated with AuNC@ZIF-8 and Hoechst 33342 or Rhodamine 123 for 1 h. Image of Hoechst 33342 obtained with band path of 420-450 nm upon excitation at 405 nm (blue) (A), image of Rhodamine 123 obtained with band path of 500-540 nm upon excitation at 488 nm (green) (B), image of AuNC@ZIF-8 obtained with band path of 560-650 nm upon excitation at 488 nm (orange) (C), and merged image (D). Scale bars: 10 μm.

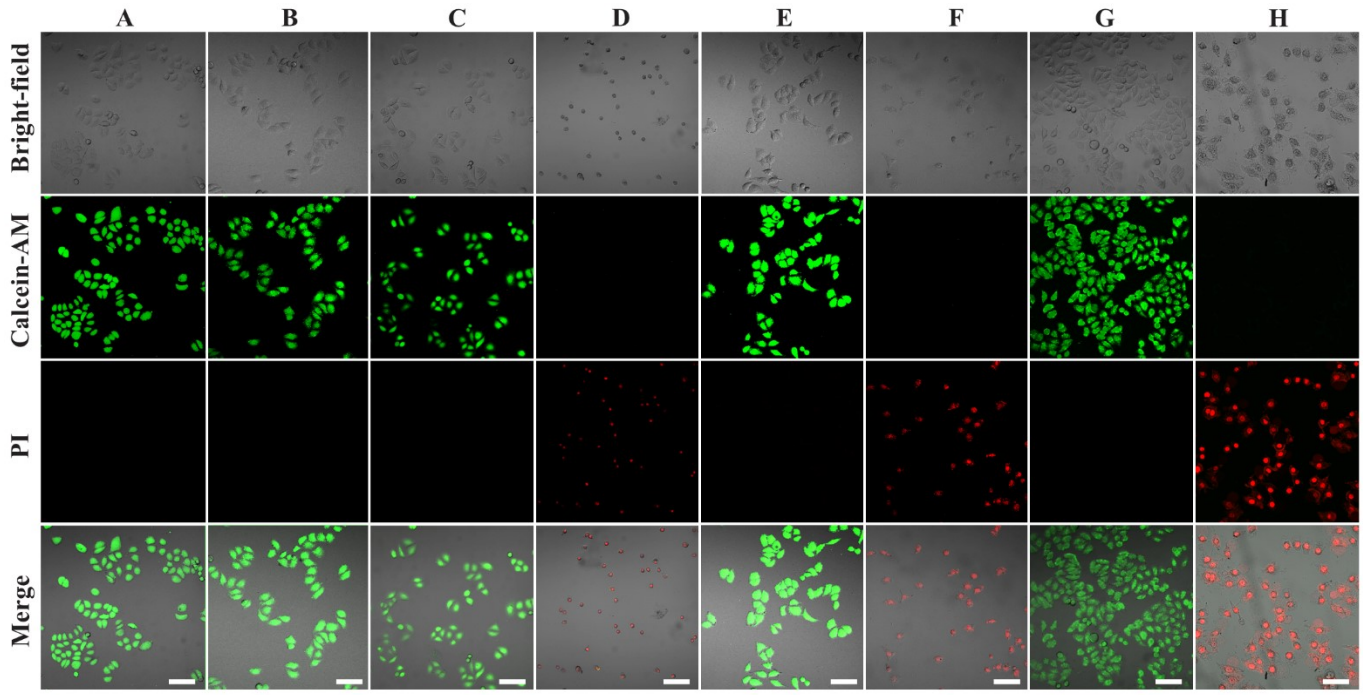

Fig. S21 CLSM images of HeLa cells after different treatments: (A) HeLa cells incubated with PBS only; (B) HeLa cells treated with light irradiation only; HeLa cells incubated with cisplatin-AuNC@ZIF-8 (50 μg/mL) and then treated without (C) and with (D) light irradiation for 5 min; HeLa cells incubated with DTX-AuNC@ZIF-8 (50 μg/mL) and then treated without (E) or with (F) light irradiation for 5 min; HeLa cells incubated with DOX-AuNC@ZIF-8 (50 μg/mL) and then treated without (G) or with (H) light irradiation for 5 min. The cells are all co-contained by Calcein-AM (green, live cells) and PI (red, dead cells). Scale bar: 50 μm.

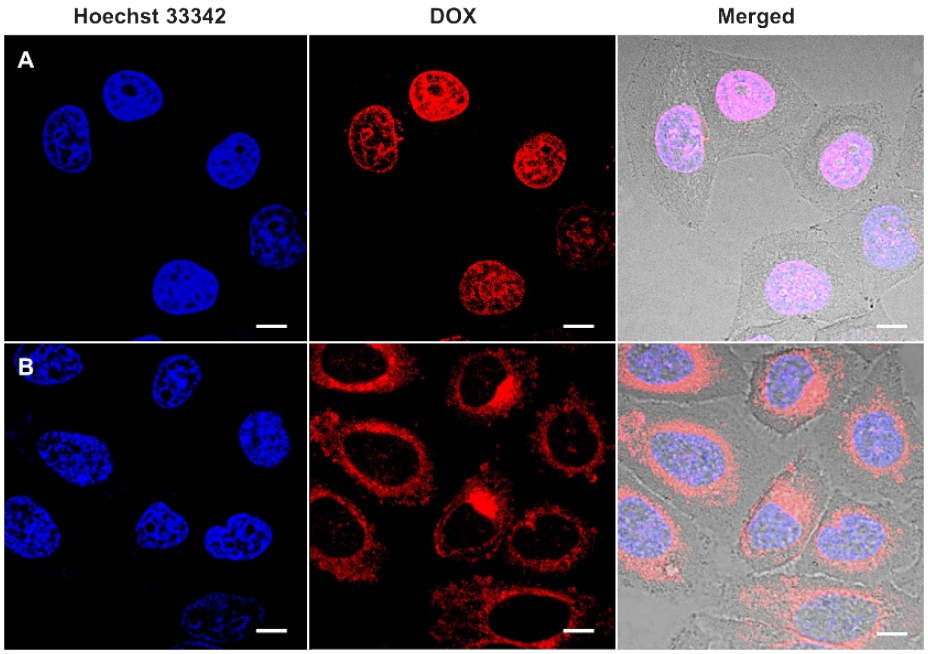

Fig. S22 CLSM images of HeLa cells incubated with free DOX (A) and DOX-AuNC@ZIF-8 (B). Scale bar: 20 μm.

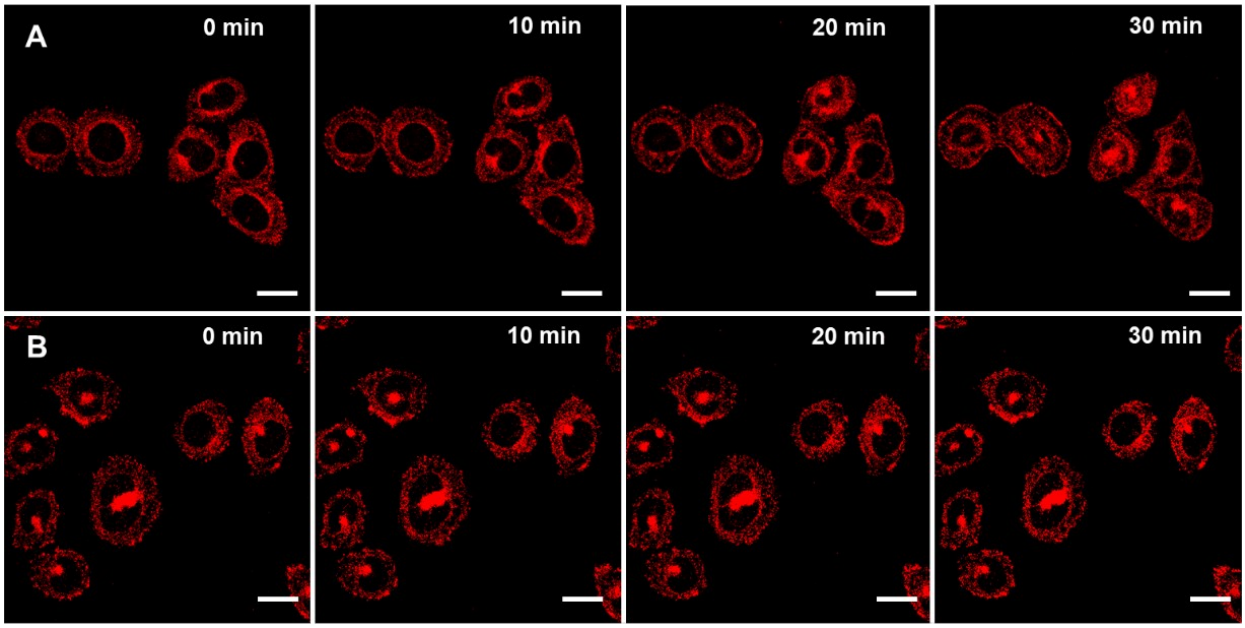

Fig. S23 CLSM images of HeLa cells incubated with DOX-AuNC@ZIF-8 with (A) or without (B) light irradiation for 5 min. Scale bar: 20 μm.

References

[1] R. Tian, S. Zhang, M. Li, Y. Zhou, B. Lu, D. Yan, M. Wei, D. G. Evans, X. Duan, Localization of Au nanoclusters on layered double hydroxides nanosheets: confinement-induced emission enhancement and temperature-responsive luminescence, Adv. Funct. Mater. 25 (2015) 5006–5015, https://doi.org/10.1002/adfm.201501433.

[2] R. Tian, D. Yan, C. Li, S. Xu, R. Liang, L. Guo, M. Wei, D. G. Evans, X. Duan, Surface-confined fluorescence enhancement of Au nanoclusters anchoring to a two-dimensional ultrathin nanosheet toward bioimaging, Nanoscale 8 (2016) 9815–9821, https://doi.org/10.1039/C6NR01624C.

[3] T. Zhao, N. Goswami, J. Li, Q. Yao, Y. Zhang, J. Wang, D. Zhao, J. Xie, Probing the microporous structure of silica shell via aggregation-induced emission in Au(I)-thiolate@SiO_2 nanoparticle, Small 12 (2016) 6537–6541, https://doi.org/10.1002/smll.201601420.

[4] F. Cao, E. Ju, C. Liu, W. Li, Y. Zhang, K. Dong, Z. Liu, J. Ren, X. Qu, Encapsulation of aggregated gold nanoclusters in a metal–organic framework for real-time monitoring of drug release, Nanoscale 9 (2017) 4128–4134, https://doi.org/10.1039/C7NR00073A.

[5] Q. Gao, S. Xu, C. Guo, Y. Chen, L. Wang, Embedding nanocluster in MOF via crystalline ion-triggered growth strategy for improved emission and selective sensing, ACS Appl. Mater. Interfaces 10 (2018) 16059–16065, https://doi.org/10.1021/acsami.8b04531.